INFLUENCES OF FIBERS ON DRYING SHRINKAGE OF FIBER-REINFORCED CEMENTITIOUS COMPOSITE

By Jun Zhang[1] and Victor C. Li,[2] Fellow, ASCE

ABSTRACT: An analytical model has been formulated for the drying shrinkage performance of a fiber-reinforced cementitious composite. The model is based on the assumption that shear stress is produced between the fiber and surrounding matrix as the matrix shrinks. This shear stress in turn influences the matrix deformation behavior resulting in macroscopic composite shrinkage lower than that of a pure cement-based matrix. Through systematic derivation, a free shrinkage expression, which reflects the influences of the matrix and fiber properties as well as fiber orientation characteristics, is presented. A parametric study, including the influence of elastic moduli of the fiber and matrix, fiber dimension, and fiber content in the case of 3D fiber distribution, is carried out. The model results indicate that shrinkage of a fiber-reinforced cement-based composite is significantly influenced by elastic moduli of fiber and matrix as well as fiber length and thickness (i.e., diameter for fiber with a circular cross section). Model predictions based on independent parametric inputs compare favorably with experimental measurements of free shrinkage of fiber-reinforced mortar and concrete.

INTRODUCTION

Drying shrinkage is probably the most deleterious property of portland cement concrete (Neville 1994). Shrinkage generally leads to cracking in concrete structures and further influences the service life of structures. This is particularly true in the case of slabs, such as concrete bridge decks and highway pavements, which have much larger surface areas compared with other kinds of structural members, such as beams and columns. Cracking in concrete slabs reduces the load capacity and has been linked to fatigue failure (Matsui 1997; Perdikaris and Beim 1988; Perdikaris et al. 1989; Kumar and GangaRao 1998). In addition, cracks allow water and other chemical agents, such as deicing salt, to penetrate the concrete cover to come into contact with the steel reinforcements, leading to reinforcement corrosion and rupture.

Hardened cement paste undergoes high drying shrinkage, whereas concrete shows significantly less shrinkage due to the restraint provided by the more rigid aggregate particles. The restrain provided by aggregate particles to the shrinkage of concrete is well understood, and theoretical models have been successfully developed (Pickett 1954; Xi and Jennings 1997). The introduction of fibers also leads to reduction in the shrinkage of the cementitious matrix. This phenomenon has been well recognized and extensively studied experimentally (Swamy and Stavrides 1979; Balaguru and Ramakrishnan 1988; Mangat and Azari 1988; Filho and Sanjuan 1999). However, the mechanism of restrain provided by the fibers is not the same as in the case of coarse aggregate particles, due to their high aspect ratio characteristics. At present, little work has been done in quantifying the links between fundamental micromaterial parameters and macrocomposite shrinkage performance.

There are two major motivations to develop a shrinkage model for fiber-reinforced cementitious composities. One is to guide the optimization of material shrinkage behavior by tailoring the types and forms of reinforcing fibers, and the other is to predict the composite shrinkage response of products or structures made of such materials. Mangat and Azari (1984) developed a model to predict the influence of steel fibers on composite shrinkage. The model needs to calculate the frictional coefficient between the fiber and matrix from free shrinkage experimental data. In this paper, an analytical model for predicting the shrinkage performance of the fiber-reinforced cementitious composite is constructed based on the shear-lag theory developed by Cox (1952) and taking into account the random nature of fiber distribution. The model incorporates material parameters of reinforcing fiber and matrix, such as elastic modulus and geometry of fiber as well as the cement/concrete matrix shrinkage performance.

In the following section, the development of the model with some basic assumptions is presented first. Then, a parametric study is given. Discussions on the influences of material properties, such as the elastic moduli ratio of the fiber and matrix, fiber aspect ratio, and fiber content, on the composite shrinkage behavior are presented in this section. Finally, model-predicted composite shrinkage performance in terms of free shrinkage-age diagrams is compared with experimental results from free shrinkage tests. Conclusions are made at the end of this paper.

PROBLEM MODELING

As the matrix shrinks, a shear stress along the fiber and matrix interface is developed. The fiber is subjected to compression, and the matrix is subjected to tension. The shrinkage of the matrix in any direction can be considered to be restrained by an aligned fiber of effective length parallel to the direction of the shrinkage strain (Mangat and Azari 1984). Before introducing the model, it is first assumed that the restraint provided by the randomly oriented fibers with length l_f and volume content V_f in the cementitious matrix is equivalent to the restraint in an idealized composite with aligned fiber distribution and effective fiber length L_{fe} and fiber spacing $2R$ (Fig. 1).

Effective Fiber Length

To solve for the effective fiber length L_{fe}, one starts by considering the averaged projected fiber length in the direction of material shrinkage. By introducing the probability density function $f(\varphi)$, defined as the ratio between the amount of fiber with orientation angle φ and the total amount of fiber in a given volume, the amount of fibers within φ to $\varphi + d\varphi$ in a unit volume of composite is given is given by

$$dV_f = V_f f(\varphi) d\varphi \tag{1}$$

[1]Postdoctoral Res. Fellow, ACE-MRL, Dept. of Civ. and Envir. Engrg., Univ. of Michigan, Ann Arbor, MI 48109-2125.

[2]Prof. and Dir., ACE-MRL, Dept. of Civ. and Envir. Engrg., Univ. of Michigan, Ann Arbor, MI.

Note. Associate Editor: Arup Maji. Discussion open until June 1, 2001. To extend the closing date one month, a written request must be filed with the ASCE Manager of Journals. The manuscript for this paper was submitted for review and possible publication on March 22, 2000. This paper is part of the ***Journal of Engineering Mechanics***, Vol. 127, No. 1, January, 2001. ©ASCE, ISSN 0733-9399/01/0001-0037–0044/$8.00 + $.50 per page. Paper No. 22274.

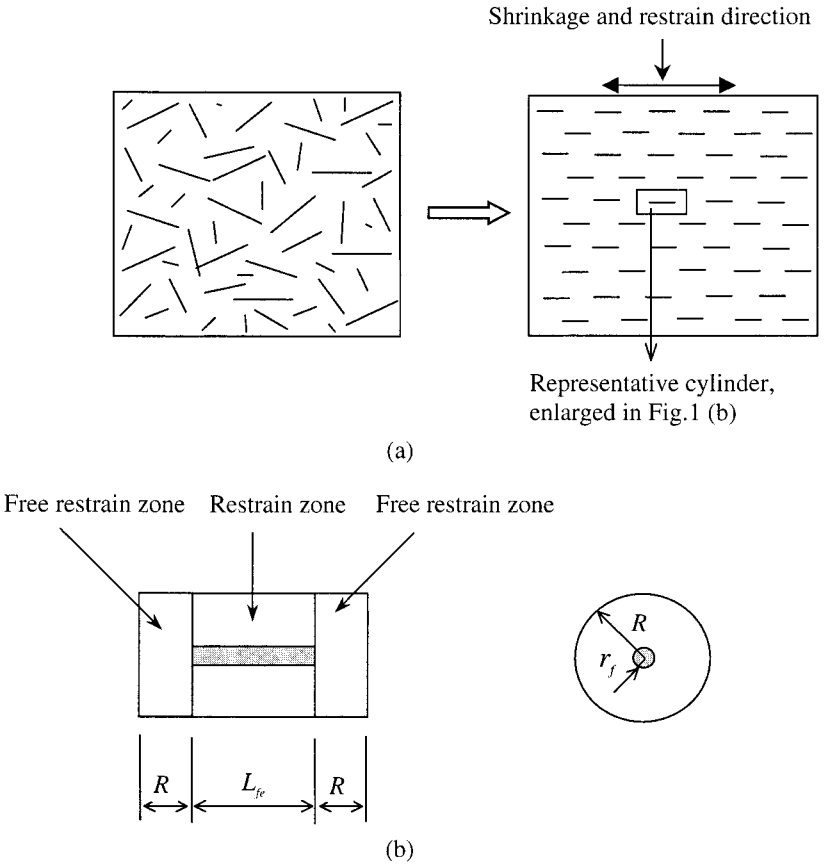

FIG. 1. Schematic Diagram Showing: (a) Equivalent Elements in Typical Fiber-Reinforced Composite; (b) Enlarged Representative Cylinder Used in This Analysis

where $f(\varphi)$ is governed by the dimension of fiber distribution; and $f(\varphi)$ is equal to $1/\pi$ and $\sin\varphi$, respectively, in 2D and 3D fiber distribution (Krenchel 1975; Li et al. 1991). Hence, the number of fibers at angle φ to $\varphi + d\varphi$ in a unit volume of composite dN is given by

$$dN = \frac{dV_f}{A_f l_f} = \frac{V_f}{A_f l_f} f(\varphi) d\varphi \tag{2}$$

where A_f = single fiber cross-sectional area. Therefore, the total projected length of fibers in the direction parallel to direction of shrinkage within φ and $\varphi + d\varphi$ in the unit volume is

$$dL_{t\varphi} = l_f dN \cos\varphi = \frac{V_f}{A_f} \cos\varphi f(\varphi) d\varphi \tag{3}$$

Then the effective fiber length, defined as the average fiber projected length in the direction parallel to direction of shrinkage, can be obtained from

$$L_{fe} = \frac{\int_\varphi dL_{t\varphi}}{\int_\varphi dN} = l_f \int_\varphi \cos\varphi f(\varphi) d\varphi = k l_f \tag{4}$$

where k = dimensional influence factor. The integration limits of φ is dependent on the dimension of fiber orientation.

In the case of 1D fiber distribution, $\varphi = 0$, then one has $L_{fe} = l_f$ ($k = 1$). Substituting $f(\varphi)$ with $1/\pi$ and $\sin\varphi$, respectively, and $\varphi \in (-\pi/2, \pi/2)$ and $\varphi \in (0, \pi/2)$ in (4), one can obtain the effective fiber restrain length in 2D and 3D fiber distribution as

$$L_{fe} = \frac{2}{\pi} l_f \quad \text{for 2D} \tag{5a}$$

$$L_{fe} = \frac{1}{2} l_f \quad \text{for 3D} \tag{5b}$$

where a circular fiber cross section is assumed.

Fiber Spacing

The fiber spacing can be obtained by the following procedure. Fig. 1(b) shows a representative cylinder element with radius R and length (L_{fe} + 2R) isolated from the aligned fiber-reinforced composite. It is assumed that the total volume of the composite is equal to the sum of all individual cylinder volumes V_{f0}, each of which contains one single fiber. In a unit volume of material containing N_0 fibers, one has

$$N_0 V_{f0} = 1 \tag{6}$$

The parameter N_0 can be expressed in terms of fiber volume fraction and fiber dimension as

$$N_0 = \frac{V_f}{\pi r_f^2 l_f} \tag{7}$$

where r_f = fiber radius. Also

$$V_{f0} = \pi R^2 (L_{fe} + 2\mathrm{R}) \tag{8}$$

Substituting N_0 and V_{f0} in (6) with (7) and (8), respectively, leads to the following expression:

$$R^2 \left(1 + \frac{2R}{k l_f}\right) = \frac{r_f^2}{k V_f} \tag{9}$$

Eq. (9) provides the general relation between fiber spacing and fiber content, fiber radius, fiber length, and fiber orientation factor. For a given composite, the fiber spacing $2R$ can be easily obtained by solving the above equation.

It is noted that as $2R/kl_f \ll 1$, (9) becomes $R = r_f/(kV_f)^{1/2}$, which is identical to the model obtained by Krenchel (1975) and Romualdi and Mandel (1964). For example, assume $2R/kl_f \leq 0.02$, then one has $kl_f/2r_f \geq 50/(kV_f)^{1/2}$. For a 2% fiber content (in volume) three-dimensionally orientated in the matrix, the above requirement leads to $l_f/2\ r_f \geq 1{,}000$. For the general short fiber-reinforced cementitious composite, this condition is not fulfilled. Therefore, (9) has to be used, in general, to calculate the parameter R.

Free Shrinkage Model of Fiber-Reinforced Cementitious Composite

The restrain provided by fibers in cement-based composite can be calculated from the representative element shown in Fig. 1(b), which is a cylinder with diameter 2R and length (L_{fe} + 2R), reinforced by a single aligned fiber with fiber length L_{fe} and diameter $2r_f$ in center. The shrinkage of the cylindrical matrix adjacent to the fiber is considered to be influenced by the fiber, whereas the left and the right parts of length R each are assumed to be free of the fiber influence.

It is assumed that the matrix is subjected to a tensile stress σ_{ma} within the restrain zone due to the restrain provided by the fiber during matrix shrinkage. Tensile stress σ_{ma} is a function of location x (Fig. 2), Thus the expression of free shrinkage of fiber-reinforced composite is given by

$$\varepsilon_t = \varepsilon_m - \frac{1}{L_{fe} + 2R} \int_0^{L_{fe}} \frac{\sigma_{ma}}{E_m}\, dx \tag{10}$$

where ε_t and ε_m = shrinkage strain of composite and pure matrix, respectively; and E_m = elastic modulus of matrix. In calculating the stress field developed in the representative cylinder due to matrix shrinkage deformation, several simplifying assumptions are made: (1) The matrix and reinforcing fiber are both elastic materials; (2) the interface between the matrix and fiber is infinitesimally thin; (3) there is no slip between the fiber and the matrix at the interface; and (4) the shrinkage strain in the matrix at a radical distance R from the fiber in the fiber axial direction is equal to the free shrinkage strain of the matrix ε_m.

When the matrix is subjected to a shrinkage strain ε_m in the direction of the reinforcing fiber, the equilibrium of the axial stress σ_f in fiber and the matrix/fiber interfacial shear stress τ_0 requires

$$\frac{\partial \sigma_f}{\partial x} + \frac{2}{r_f}\,\tau_0 = 0 \tag{11}$$

Further differentiation of (11) with respect to x results in

$$\frac{\partial^2 \sigma_f}{\partial^2 x} + \frac{2}{r_f}\,\frac{\partial \tau_0}{\partial x} = 0 \tag{12}$$

From shear-lag theory (Cox 1952), the interfacial shear stress can be expressed as

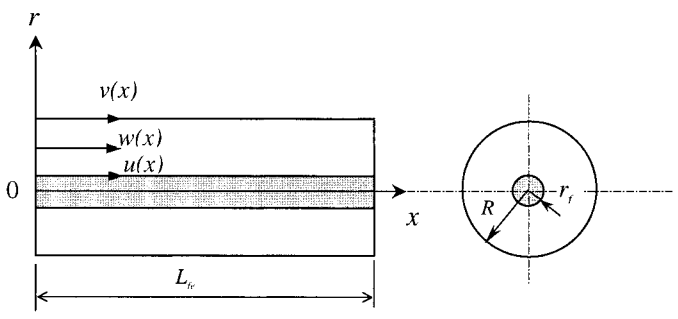

FIG. 2. Schematic Drawing of Shear-Lag Model Used in Analyzing Stress Transfer from Fiber to Matrix during Matrix Shrinking

$$\tau_0 = \frac{E_m}{2(1 + \nu_m)}\,\frac{v - u}{r_f \log(R/r_f)} \tag{13}$$

where v and u = displacement field at $r = R$ and $r = r_f$, respectively (Fig. 2). Hence

$$\frac{\partial \tau_0}{\partial x} = \frac{E_m}{2(1 + \nu_m) r_f \log(R/r_f)} \left(\varepsilon_m - \frac{\sigma_f}{E_f}\right) \tag{14}$$

Replacing $\partial\tau_0/\partial x$ with (14) in (12), the general equation governing the axial stress distribution in reinforcing fiber σ_f is

$$\frac{\partial^2 \sigma_f}{\partial^2 x} + \frac{E_m}{r_f^2(1 + \nu_m)}\,\frac{1}{\log(R/r_f)} \left(\varepsilon_m - \frac{\sigma_f}{E_f}\right) = 0 \tag{15}$$

To solve this differential equation with boundary conditions in which $\sigma_f = 0$ at $x = 0$ and $x = L$ yields:

$$\sigma_f = E_f \varepsilon_m \left[1 - \frac{\cosh \beta \left(\dfrac{L - 2x}{2r_f}\right)}{\cosh \beta\, \dfrac{L}{2r_f}}\right] \tag{16}$$

where

$$\beta = \sqrt{\frac{E_m}{(1 + \nu_m) E_f \log(R/r_f)}} \tag{17}$$

Eqs. (14) and (16) indicate that the shrinkage strain ε_m drives the interfacial shear stress and fiber stress. Recognizing that the net axial force in the free restrain zone is zero, mechanical equilibrium of the external load and internal stress distributions at any location x requires

$$\sigma_f A_f + 2\pi \int_{r_f}^{R} \sigma_m r\, dr = 0 \tag{18}$$

where σ_m = axial stress in the matrix, which is a function of r. Introducing an average stress in the matrix, σ_{ma} defined by

$$\sigma_{ma} = \frac{2\pi \displaystyle\int_{r_s}^{R} \sigma_m r\, dr}{A_m} \tag{19}$$

(18) can be rewritten

$$\sigma_f A_f + \sigma_{ma} A_m = 0 \tag{20}$$

where A_f and A_m = cross-sectional areas of reinforcing fiber and matrix, respectively. Replacing σ_f with (16) in (20), the average stress in the matrix as a function of location x can be given by

$$\sigma_{ma} = -\frac{A_f}{A_m} E_f \varepsilon_m \left[1 - \frac{\cosh \beta \left(\dfrac{L - 2x}{2r_f}\right)}{\cosh \beta\, \dfrac{L}{2r_f}}\right] \tag{21}$$

The first negative sign in (21) indicates that the matrix stress is opposite to that in the fiber. The volume shrinkage of the cementitious matrix imposes a compressive stress on the reinforcing fibers and a tensile stress on the matrix itself.

Substituting σ_{ma} in (10) with (21), the shrinkage of fiber-reinforced composite is expressed as

$$\varepsilon_t = \varepsilon_m \left[1 - \eta\, \frac{kV_f}{1 - kV_f(1 + 1/\gamma_1)} \left(1 - \frac{1}{\beta\gamma} \tanh \beta\gamma\right)\right] \tag{22}$$

where

$$\eta = \frac{E_f}{E_m}; \quad \gamma = \frac{kl_f}{2r_f}; \quad \gamma_1 = \frac{kl_f}{2R}$$

$$\beta = \left(\frac{1}{(1 + \nu_m)\eta \log \gamma_2}\right)^{1/2}; \quad \gamma_2 = \left(\frac{1}{kV_f(1 + 1/\gamma_1)}\right)^{1/2}$$

Eq. (22) provides a general expression of free shrinkage of fiber-reinforced cementitious composite. The influences of fiber properties, including fiber length, diameter, and elastic modulus, and matrix properties, including its free shrinkage behavior and elastic modulus, as well as fiber content and fiber distribution characteristic in the matrix are fully reflected. It is noted that when the second term inside the square brackets in (22) achieves its maximum value of 1, the shrinkage of the composite becomes zero. This means that the matrix shrinkage if fully compensated by restrain of the fibers. However, it should be noted that overrestrain of reinforcements to matrix shrinkage may result in cracking in the matrix (Zhang et al. 2000). As described above, the matrix is subjected to tensile stress due to restrain of fibers. The maximum tensile stress generated in the matrix needs to be calculated from (21) and compared to its tensile strength in order to prevent cracking in the matrix (i.e., if the tensile stress in the matrix is over the matrix tensile strength, the fiber geometry and content may need to be adjusted).

In addition, by taking limit analysis as $\gamma \to \infty$, (i.e., $l_f \to \infty$ or $r_f \to 0$), (22) becomes

$$\varepsilon_t = \varepsilon_m \left(1 - \eta \frac{kV_f}{1 - kV_f}\right) \tag{23}$$

In this case, free shrinkage of the composite is only influenced by the ratio of fiber to matrix moduli, fiber volume concentration, and fiber orientation characteristic. To fully compensate the matrix shrinkage, the fiber volume content, called the critical fiber content V_f^{crit} can be calculated by

$$V_f^{\text{crit}} = \frac{1}{k(1 + \eta)} \tag{24}$$

The influence of moduli ratio η on V_f^{crit} is graphically shown in Fig. 3, where three typical fiber orientation characteristics are present. Increasing the moduli ratio of the fiber and matrix is an effective way to compensate for matrix shrinkage in fiber-reinforced cementitious composites. As expected, less fiber is needed to compensate a given shrinkage strain as fibers tend to parallel the direction of matrix shrinking (i.e., from three dimensions to one dimension).

PARAMETRIC STUDY

In this section, the influences of material parameters of both fiber and matrix on the free shrinkage of fiber-reinforced cement-based composite are investigated. As cement-based matrix properties, the free shrinkage strain ε_m and elastic modulus E_m are time dependent. The following empirical expressions, which describe the time-dependent law of the above parameters, are used in the present analysis.

Long-term studies (Branson 1977) show that, for moisture-cured concrete or mortar at any time t (in days), shrinkage can be predicted satisfactorily by

$$\varepsilon_{m,t} = \frac{t}{35 + t} \varepsilon_{m,u} \tag{25}$$

where $\varepsilon_{m,t}$ = free shrinkage strain at time t (in days); and $\varepsilon_{m,u}$ = ultimate value after a long period of time, which is governed by mix proportions and specimen curing conditions. The time-dependent law of the elastic modulus of concrete and mortar can by estimated by (Mosley and Bungey 1990)

$$E_{m,t} = E_{m,28}[0.52 + 0.15 \log(t)] \quad \text{for } t \le 28 \tag{26a}$$

$$E_{m,t} = 1.019E_{m,28} \quad \text{for } t > 28 \tag{26b}$$

where $E_{m,t}$ and $E_{m,28}$ = elastic moduli at time t days and 28 days, respectively. Elastic modulus $E_{m,28}$ may be determined from experiments or estimated from existing models, such as that given by Hasin (1962). His model allows calculation of the modulus of the cementitious matrix according to the mix proportions and modulus of cement paste.

Influence of Elastic Moduli of Fiber and Matrix

The influence of the elastic moduli of the fiber and matrix on the composite free shrinkage can be identified by isolating the moduli-related parameters from (22) to form the so-called modulus influence factor K_E, defined as follows:

$$K_E = \eta \left(1 - \frac{1}{\beta\gamma} \tanh \beta\gamma\right) \tag{27}$$

Larger K_E results in smaller composite shrinkage strain. It is clear from (27) that K_E increases with an increase in moduli ratio η. In addition, the value β is also a function of η, [see (17)]. Therefore, it is not a simple linear relationship between K_E and η. As an example, it is assumed that 3% (in volume) fiber with 28.2 mm in length and 0.48 mm in diameter is used in mortar. The fibers are three-dimensionally randomly orientated in the matrix. It is further assumed that $E_{m,28}$ = 20 GPa and $\varepsilon_{m,u} = 1{,}150 \times 10^{-6}$. Fig. 4 shows the influence of the moduli ratio on the factor K_E in terms of the $K_E - \eta$ diagram.

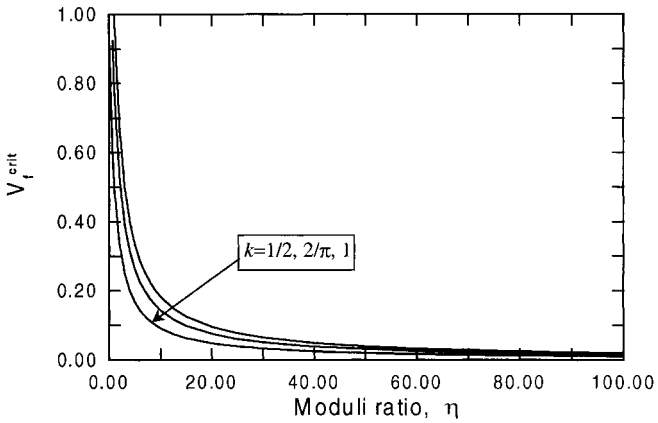

FIG. 3. Theoretical Relationship between Critical Fiber Content and Modulus Ratio of Fiber and Matrix

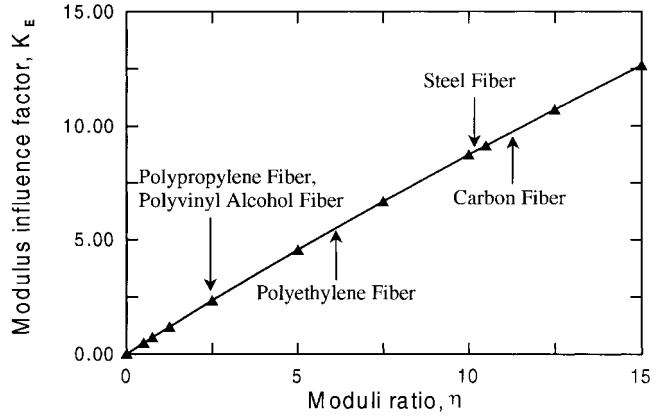

FIG. 4. Relationship between Modulus Influence Factor and Modulus Ratio

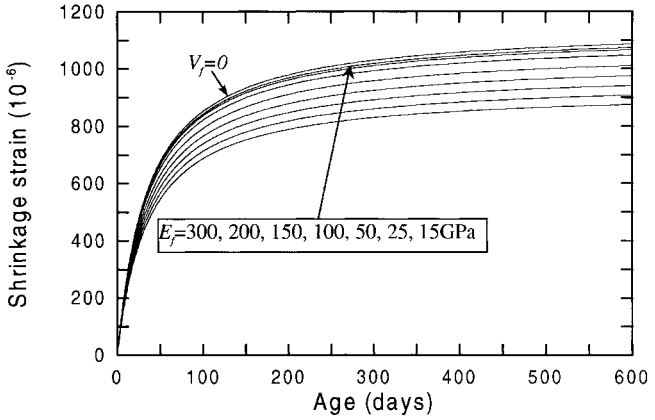

FIG. 5. Influence of Fiber Modulus on Composite Shrinkage Performance

The typical influence of the fiber elastic modulus (E_f changed from 300 to 15 GPa) on the composite shrinkage behavior in terms of free shrinkage strain versus age curves is shown in Fig. 5. It is obvious that increasing the fiber modulus or reducing the matrix modulus can raise the efficacy of fibers with respect to the restrain on the matrix shrinkage. Based on this result, it can be concluded that high modulus fibers, such as steel and carbon fibers, are more effective than low modulus fibers, such as polypropylene and polyvinyl alcohol fibers, in reducing the matrix shrinkage under the same fiber content and fiber geometry. In addition, fibers in immature cementitious matrix are more effective on the restrain to the matrix shrinkage than that in the matured matrix due to the difference in the matrix elastic modulus.

Influence of Fiber Aspect Ratio

The influence of fiber aspect ratio can be described by the parameter γ in (22), which may be called the effective fiber aspect ratio because the dimensional influence factor k is involved. Similar to the above analysis, the fiber-aspect-ratio-related terms in (22) form the fiber aspect ratio influence factor K_γ, defined as follows:

$$K_\gamma = \frac{1}{1 - kV_f(1 + 1/\gamma_1)}\left(1 - \frac{1}{\beta\gamma}\tanh \beta\gamma\right) \qquad (28)$$

It is noted that γ_1 is a function of γ [see (9)]. Therefore, γ_1-related terms in (22) are also included in (28). From (28), it can be found that K_γ increases with the increase of γ. However, as $\gamma \to \infty$ ($l_f \to \infty$ or $r_f \to 0$), $K_\gamma = 1/(1 - kV_f)$. This is the upper limitation of the factor K_γ, which is independent of fiber geometry and only influenced by fiber content and distribution characteristic.

As an example, it is assumed that steel fiber with a different fiber aspect ratio is used separately in the mortar. The fibers are 3D orientated in the matrix. It is further assumed that E_m = 20 GPa and E_f = 210 GPa. Fig. 6 shows the relationship between the factor K_γ and the effective fiber aspect ratio γ for different fiber content. The triangle marks indicate the points at which the factor K_γ achieves 98% of its upper limit. The corresponding aspect ratio is called the critical fiber aspect ratio regarding shrinkage reduction. From this relationship, first it can clearly be seen that K_γ increases nonlinearly with the increase of γ. To reduce composite shrinkage, fibers with a high aspect ratio are more effective than those with a low aspect ratio. The development of the factor K_γ with the fiber aspect ratio γ can be characterized by a rapidly increasing stage followed by a slowly increasing stage. An upper limit of the factor K_γ exists. Second, the range of γ in each stage is influenced by fiber content. With the increase of fiber content,

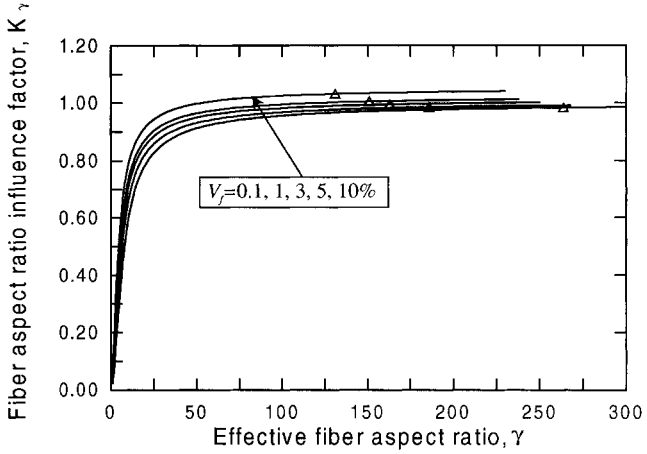

FIG. 6. Influence of Fiber Aspect Ratio on Factor K_γ, Showing Different Fiber Content

the first stage becomes increasingly shorter and the second stage moves forward gradually. The same tendency is found on the critical fiber aspect ratio (Fig. 6). This indicates that short fibers (fiber length is one of the critical fiber parameters for uniformly dispersing fibers in the matrix) may be selected with an increasing fiber content without reducing the efficiency with respect to the matrix shrinkage reduction. Careful selection on fiber geometry is necessary in order to reduce dry shrinkage of the fiber-reinforced cement-based composite.

Influence of Fiber Content

The influence of fiber content on composite shrinkage is reflected by V_f itself and V_f dependent parameters γ_1 and β. Thus, the fiber content influence factor is given by

$$K_V = \frac{kV_f}{1 - kV_f(1 + 1/\gamma_1)}\left(1 - \frac{1}{\beta\gamma}\tanh \beta\gamma\right) \qquad (29)$$

To analyze the fiber content influence on factor K_V, it is assumed that steel fibers 28.2 mm in length and 0.48 mm in diameter are three-dimensionally orientated in mortar. It is further assumed that $E_{m,28}$ = 20 GPa, E_f = 210 GPa, and $\varepsilon_{m,u}$ = 1,150 $\times$ 10^{-6}. Fig. 7 shows the relationship between K_V and V_f. As expected, K_V increases with the increase of the fiber content. Fig. 8 demonstrates a typical theoretical relationship between free shrinkage and fiber content in terms of composite shrinkage strain versus age diagrams. The more the fiber is added, the less the composite shrinkage strain generates. However, in practice, processing technology and fiber price may also govern the fiber content in the matrix. Synthetic consid-

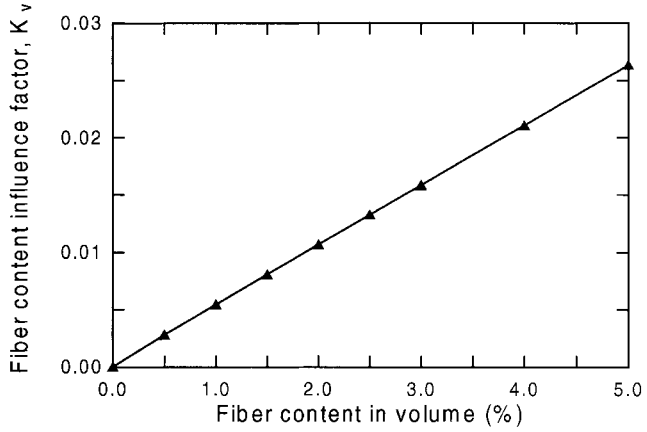

FIG. 7. Influence of Fiber Content on Factor K_V

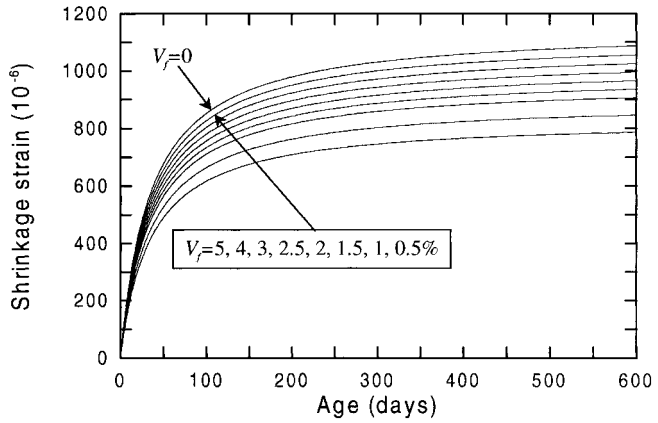

FIG. 8. Influence of Fiber Content on Composite Shrinkage Behavior

erations on fiber content regarding composite shrinkage are necessary.

EXPERIMENTAL VERIFICATION

An investigation on free shrinkage performance of steel fiber-reinforced mortar and concrete had been carried out by Mangat and Azari (1988). The experimental results obtained by the above study are compared with the model predictions. The experimental details are briefly summarized as follows.

Shrinkage tests were carried out on concrete and mortar reinforced with different kinds of steel fibers. Ordinary portland cement, fine aggregate conforming to Zone 2 of British Standard 882, and granite coarse aggregate of 10-mm normal size were used throughout. Three types of steel fibers (i.e., melt extract, crimped, and hooked steel fibers) were used separately. A concrete mix of proportions by weight of 1:2.5:1.25:0.58, (cement:sand:stone:water) and a mortar mix of proportions by weight of 1:2.75:0:0.58 (cement:sand:stone:water) were used. The fiber content of the mixes ranged between 0 and 3% in volume. It should be noted that the fiber volume content in concrete is relative to the mortar constituents of the mix, with the volume of coarse aggregate being excluded. Two prism specimens with dimensions of 100 × 100 × 500 mm were cast for each mix. The specimens were cast horizontally in three layers, and the concrete was well compacted on a vibrating table. The surface of the specimens was covered with a plastic sheet after casting and cured for 24 h at room temperature. Then the specimens were removed form their molds and put into a temperature and humidity controlled room where a temperature of 20°C and a relative humidity of 55% were maintained. Free shrinkage was measured by means of a Demec extensometer over a gauge length of 200 mm. The first measurement was taken at 24 h after casting and regular measurements were made thereafter up to 120 or 520 days age. It should be pointed out that the writers also presented some free shrinkage results of the fiber-reinforced concrete under an uncontrolled laboratory air curing condition. In the present study, those experimental results are not selected to compare with the model predictions because some unexpected factors that may influence the shrinkage test results may be included in this case. [A more detailed description of the experiments can be found in Mangat and Azari (1988).]

The related material parameters of the above-mentioned fiber-reinforced concrete and mortar used in the model calculations are summarized in Table 1. It should be noted that the matrix elastic moduli at 28 days of concrete and mortar for model input are the same, because, even in concrete, fibers are always surrounded with mortar. In fact, the restrain provided by the fibers acts on their surrounded mortar. Of course, the restrain to mortar finally results in reducing the free shrinkage of concrete. The influence of coarse aggregates on the free shrinkage of concrete is independently involved in the term of matrix free shrinkage ε_m in this study. It should be pointed out that the selection of $\varepsilon_{m,u}$ is based on the shrinkage test results on a plain matrix without fibers. In modeling, three different fiber orientation factors (from one to three dimensions, $k = 1$, $k = 2/\pi$, and $k = 1/2$) are used. Therefore, three shrinkage strain versus age diagrams are obtained in each prediction.

The comparisons between model predictions, calculated from (22), and experimental results in terms of free shrinkage strain versus casting age curves of different steel fiber-reinforced mortar and concrete are shown in Figs. 9–12. In these

TABLE 1. Material Parameters Used in Model

Matrix (1)	$E_{m,28}$ (GPa) (2)	$\varepsilon_{m,u}$ (3)	Fiber parameters (4)
Concrete	20	825×10^{-6}	Crimped—r_f = 0.57 mm; l_f = 48.7 mm (58.7 mm)[a]; E_f = 210 GPa; V_f = 0, 1, 2, and 3%
	20	$1{,}025 \times 10^{-6}$	Melt-extract—r_f = 0.20 mm; l_f = 22.5 mm; E_f = 210 GPa; V_f = 0, 1.5, and 3%
Mortar	20	$1{,}050 \times 10^{-6}$	Hooked—r_f = 0.24 mm; l_f = 28.2 mm (34.2 mm)[a]; E_f = 210 GPa; V_f = 0 and 3%
	20	$1{,}050 \times 10^{-6}$	Melt-extract—r_f = 0.20 mm; l_f = 22.5 mm; E_f = 210 GPa; V_f = 0 and 3%

[a]Fiber length used in model considering influence of crimps and hooks.

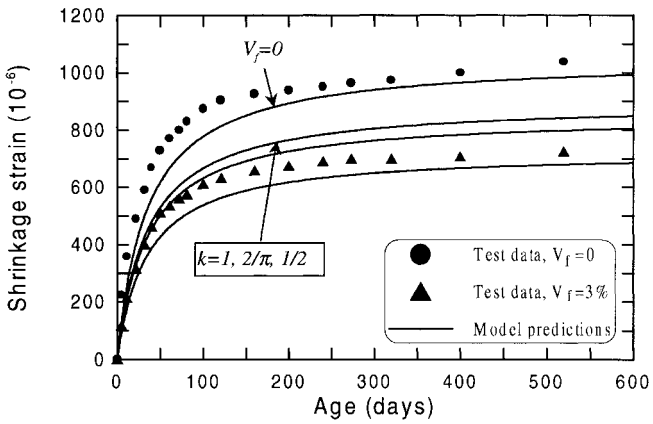

FIG. 9. Influence of Hooked Steel Fiber on Free Shrinkage Behavior of Mortar—Comparisons between Model Predictions and Experiments

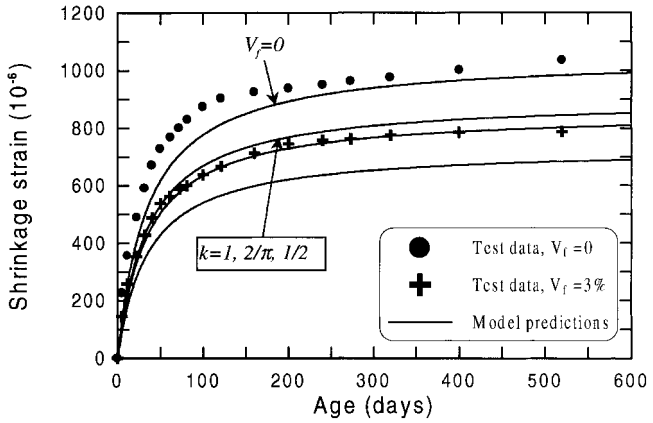

FIG. 10. Influence of Melt Extract Steel Fiber on Free Shrinkage Behavior of Mortar—Comparisons between Model Predictions and Experiments

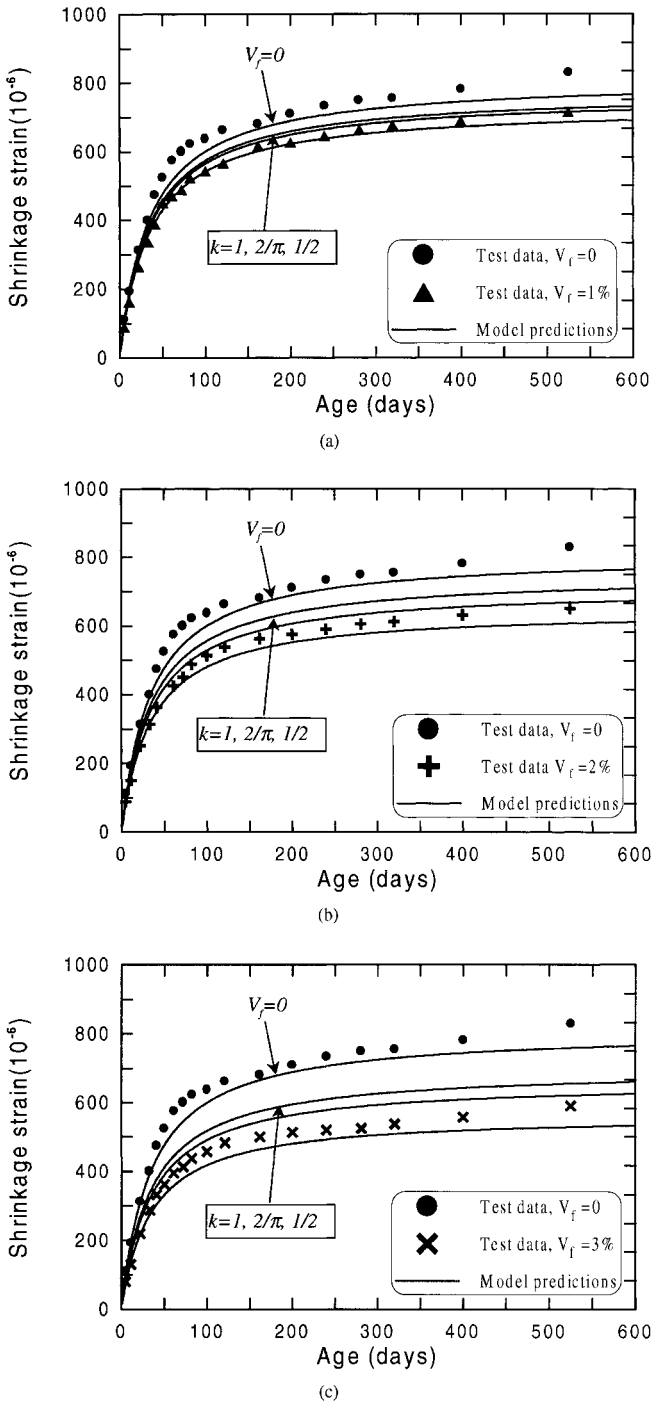

FIG. 11. Influence of Crimped Steel Fiber on Free Shrinkage Behavior of Concrete—Comparisons between Model Prediction and Experiments: (a) V_f = 1%; (b) V_f = 2%; (c) V_f = 3%

figures, first it can be seen that all of the experimental results are well located within the model predicted curves with k = 1 and k = 1/2. This is understandable because these two cases represent the extreme limits of fiber orientations in the matrix (i.e., 1D and 3D distributions). Second, most of the test results are close to the curves with $k = 2/\pi$ (2D distribution). This result may be explained as follows. As described above, the test specimens were cast horizontally in three layers, with each layer roughly 33 mm in height. In this case, the fibers 22.5–48.7 mm in length should be distributed close to two dimensions in each layer and results in 2D fiber distribution in the whole specimen. Third, as expected, fiber orientation characteristics in the matrix can significantly influence the composite shrinkage performance.

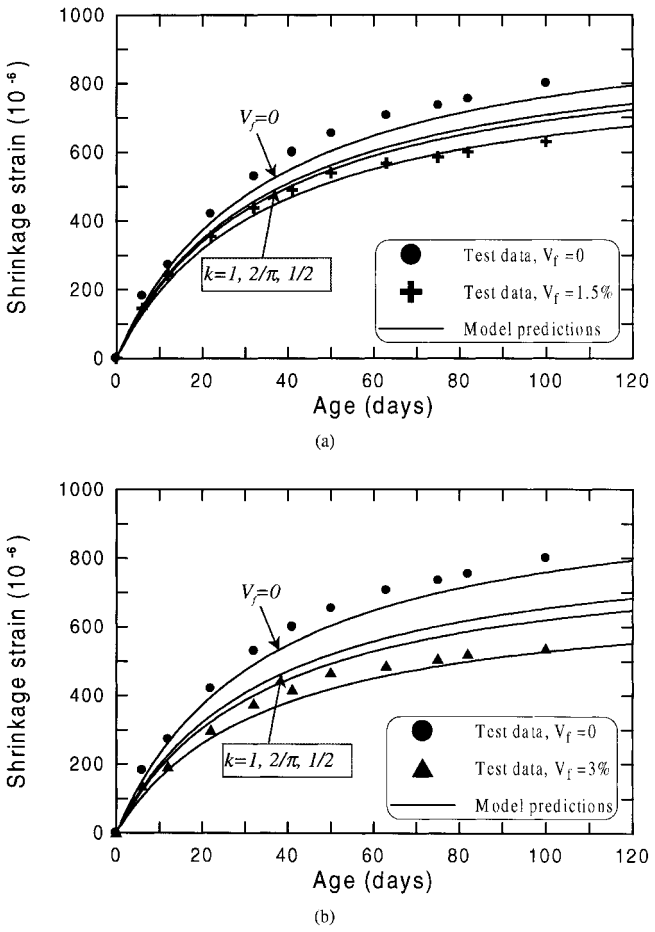

FIG. 12. Influence of Melt Extract Steel Fiber on Free Shrinkage Behavior of Concrete—Comparisons between Model Predictions and Experiments: (a) V_f = 1.5%; (b) V_f = 3%

Based on the above analysis, it can be concluded that good agreement between theoretical predictions and test results are obtained. The present model can well predict fiber influences on the shrinkage performance of cement-based fiber-reinforced composite.

CONCLUSIONS

An analytical approach for modeling the free shrinkage performance of a fiber-reinforced cementitious composite has been presented. The model relies on the shear stress transmitted between the fiber and surrounding matrix as the fundamental mechanism of restrain provided by fibers. A distinct free shrinkage expression [(22)] that reflects both matrix and fiber properties, including free shrinkage behavior of pure matrix ε_m, elastic moduli ratio of fiber and matrix η, fiber orientation characteristic k, fiber effective aspect ratio γ, and fiber content V_f, is obtained. A parametric study with the present model yields the following conclusions.

With the same fiber content and fiber geometry, the higher the moduli ratio between fiber and matrix, the smaller the composite shrinkage. High elastic modulus fibers are more effective than those with a low elastic modulus regarding composite shrinkage reduction. In addition, fiber restrain to cement matrix shrinkage may be more significant at an earlier age due to the lower elastic modulus of the matrix (and therefore higher moduli ratio η) in this stage.

The fiber aspect ratio is an important material parameter that strongly influences the composite shrinkage behavior. For the same fiber content, composite shrinkage decreases nonlinearly and gradually shifts to a constant with an increase in the fiber

aspect ratio. A critical fiber aspect ratio exists regarding a composite shrinkage reduction, and a further increase in the fiber aspect ratio beyond this critical value does not contribute to reducing the composite shrinkage. Practically speaking, a fiber aspect ratio beyond 50 has little additional effect on composite shrinkage. On the other hand, the fiber length and thickness may be limited by workability during material processing and the possibility of rupture in service. The fiber dimension should be selected during composite design with these various constraints in mind. As expected, the higher the fiber content, the lower the composite shrinkage.

Model predictions are compared with independent experimental results (Mangat and Azari 1988), and a good correlation between the model and experiments is found. The model can be used in both material optimization and performance prediction with regard to drying shrinkage of a fiber-reinforced cementitious composite.

ACKNOWLEDGMENT

This work was supported by a grant from the National Science Foundation (CMS-9872357) to the University of Michigan, Ann Arbor, Mich.

APPENDIX. REFERENCES

Balaguru, P., and Ramakrishnan, V. (1988). ''Properties of fiber reinforced concrete: Workability, behavior under long-term loading and air-void characteristics.'' *ACI Mat. J.*, 85(3), 189–196.

Branson, D. E. (1977). *Deformation of concrete structures*, McGraw-Hill, New York.

Cox, H. L. (1952). ''The elasticity and strength of paper and other fibrous materials.'' *Br. J. Appl. Phys.*, 3, 72–79.

Filho, R. D. T., and Sanjuan, M. A. (1999). ''Effect of low modulus sisal and polypropylene fiber on the restrained shrinkage of mortars at early age.'' *Cement and Concrete Res.*, 29, 1597–1604.

Hasin, Z. (1962). ''The elastic moduli of heterogeneous material.'' *J. Appl. Mech.*, 29, 143–150.

Krenchel, H. (1975). ''Fiber spacing and specific fiber surface.'' *Proc., RILEM Conf. on Fiber Reinforced Cement and Concrete*, A. Neville, ed., The Construction Press, U.K., 69–79.

Kumar, S. V. and GangaRao, H. V. S. (1998). ''Fatigue response of concrete decks reinforced with FRP rebars.'' *J. Struct. Engrg.*, ASCE, 124(1), 11–16.

Li, V. C., Wang, Y., and Backer, S. (1991). ''A micromechanical model of tension-shortening and bridging toughening of short random fiber reinforced brittle matrix composites.'' *J. Mech. Phys. Solids*, 39(5), 607–625.

Mangat, P. S., and Azari, M. M. (1984). ''A theory for the free shrinkage of steel fiber reinforced cement matrices.'' *J. Mat. Sci.*, 19, 2183–3194.

Mangat, P. S., and Azri, M. M. (1988). ''Shrinkage of steel fiber reinforced cement composites.'' *Mat. and Struct.*, Paris, 21, 163–171.

Matsui, S. (1997). ''Technology developments for bridge decks—Innovations on durability and construction.'' *Kyouryou To Kiso*, (8), 84–92 (in Japanese).

Mosley, W. H., and Bungey, J. H. (1990). *Reinforced concrete design*, Macmillan Education Ltd.

Neville, A. (1994). ''With expensive cement?'' *Concrete Int.*, 16(9), 34.

Perdikaris, P. C., and Beim, S. (1988). ''R/C bridge decks under pulsating and moving load.'' *J. Struct. Engrg.*, ASCE, 114(3), 591–607.

Perdikaris, P. C., Beim, S. R., and Bousias, S. N. (1989). ''Slab continuity effect on ultimate and fatigue strength of reinforced concrete bridge deck models.'' *ACI Struct. J.*, 86(4), 483–491.

Pickett, G. (1956). ''Effect of aggregate on shrinkage of concrete and a hypothesis concerning shrinkage.'' *J. ACI*, 27(5), 581–590.

Romualdi, J. P., and Mandel, J. A. (1964). ''Tensile strength of concrete affected by uniformly distributed and closely spaced short lengths of wire reinforcement.'' *J. ACI*, 61, 657–670.

Swamy, R. S., and Stavrides, H. (1979). ''Influence of fiber reinforcement on restraining shrinkage and cracking.'' *J. ACI*, 75, 443–460.

Xi, Y., and Jennings, H. M. (1997). ''Shrinkage of cement and concrete modeled by a multiscale effective homogeneous theory.'' *Mat. and Struct.*, Paris, 30, 329–339.

Zhang, J., Li, V. C., and Wu, C. (2000). ''Influence of reinforcing bars on the shrinkage stress in concrete slab.'' *J. Engrg. Mech.*, ASCE, 126(12), 1297–1300.